

## Measurements of total reaction cross sections for some light nuclei at intermediate energies

D. Q. Fang,<sup>1</sup> W. Q. Shen,<sup>1,2,\*</sup> J. Feng,<sup>1</sup> X. Z. Cai,<sup>1</sup> J. S. Wang,<sup>3</sup> Q. M. Su,<sup>1</sup> H. Y. Zhang,<sup>1</sup> P. Y. Hu,<sup>1</sup> Y. G. Ma,<sup>1,2</sup> Y. T. Zhu,<sup>3</sup> S. L. Li,<sup>3</sup> H. Y. Wu,<sup>3</sup> Q. B. Gou,<sup>3</sup> G. M. Jin,<sup>3</sup> W. L. Zhan,<sup>3</sup> Z. Y. Guo,<sup>3</sup> and G. Q. Xiao<sup>3</sup>

<sup>1</sup>Shanghai Institute of Nuclear Research, Chinese Academy of Sciences, Shanghai 201800, China

<sup>2</sup>CCAST (World Laboratory), P.O. Box 8730, Beijing 100080, China

<sup>3</sup>Institute of Modern Physics, Chinese Academy of Sciences, Lanzhou 730000, China

(Received 6 December 1999; revised manuscript received 9 March 2000; published 17 May 2000)

Measurements of the total reaction cross section for  $^{12-16}\text{C}$ ,  $^{14-17}\text{N}$ , and  $^{16-18}\text{O}$  on carbon target at intermediate energies were performed on the Radioactive Ion Beam Line of the Heavy Ion Research Facility in Lanzhou. A larger enhancement of  $\sigma_R$  for  $^{15}\text{C}$  was observed than for its neighbors. Evidence for possible anomalous nuclear structure in  $^{15}\text{C}$  was revealed in the analysis of the total reaction cross section in terms of the difference factor  $d$ .

PACS number(s): 25.60.Dz, 27.20.+n, 24.10.-i

### I. INTRODUCTION

Since the discovery of neutron skin and neutron halo nuclei such as  $^6\text{He}$ ,  $^8\text{He}$ ,  $^{11}\text{Li}$ ,  $^{11}\text{Be}$ ,  $^{14}\text{Be}$ ,  $^{14}\text{B}$ ,  $^{19}\text{C}$ , etc. [1–5], through several experimental methods such as measurement of the total reaction cross section, the study on the structure of nuclei far from the  $\beta$ -stability line is of particular interest regarding the possible existence of new skin and halo nuclei. It was shown that the information about such nuclear structure can be extracted from the total reaction cross section, fragment momentum distribution of fragmentation reaction, quadrupole moment and Coulomb dissociation, etc. [3–9].

Recent measurement of the interaction cross section at 960 MeV/nucleon exhibits a one-neutron halo structure of  $^{19}\text{C}$  [5]. The investigation on the Coulomb dissociation of  $^{19}\text{C}$  supports the assumption of the halo structure [10]. The measurement of the momentum distribution is also in favor of this conclusion [11]. The momentum distribution width of  $^{14}\text{C}$  from the breakup of  $^{15}\text{C}$  extracted to be  $67 \pm 3$  MeV/ $c$  is quite narrow although it is larger than the width ( $42 \pm 4$  MeV/ $c$ ) of  $^{18}\text{C}$  from the breakup of  $^{19}\text{C}$  [11]. Similar proof was demonstrated in another momentum distribution measurement [12]. So far, the extraction of the nucleon density distribution in nuclei and nuclear radii from experimental total reaction cross section has been done almost exclusively by using Glauber model. But the comparison of available data at relativistic energies and data at intermediate energies has shown great discrepancies. It was pointed out by Ozawa *et al.* that Glauber model calculation always underestimates the cross sections at intermediate energies, if one assumes harmonic-oscillator (HO)-type density distribution and determines the width parameter by reproducing the interaction cross section at relativistic energies [4]. For quantitative discussion, a difference factor  $d$  was defined as [4]

$$d = \frac{\sigma_R(\text{exp}) - \sigma_R(G)}{\sigma_R(G)}, \quad (1)$$

where  $\sigma_R(\text{exp})$  is the experimental  $\sigma_R$  at intermediate energies and  $\sigma_R(G)$  is the  $\sigma_R$  calculated by the Glauber model at the same energies with HO-type density distribution obtained by fitting the experimental  $\sigma_R$  at relativistic energy. It was shown that  $d$  is about 10–20 % for stable nuclei and nuclei near  $\beta$ -stability line. For nuclei with anomalous structure  $d$  will be 30–40 % and even up to 50%. For the large value of  $d$ ,  $^{15}\text{C}$  was suggested tentatively to have an anomalous nuclear structure (a halo or a skin) [4]. In order to draw any conclusive statements on the structure of exotic nuclei from the measured total nuclear reaction cross section at intermediate energies, the investigation on the isotope and isospin dependence of  $d$  is very important. Since only a few measurements of  $\sigma_R$  at intermediate energy range have been made, there are no clear isotope and isospin dependence of  $d$  for light exotic nuclei. Thus, more measurements of  $\sigma_R$  at intermediate energies are needed for the systematic study of the structure of light exotic nuclei.

Section II of this paper describes our experimental procedure and the data analysis method. Section III compares the experimental result with the Glauber model calculation and investigates the isotope dependence of the difference factor  $d$ . A brief summary and our conclusions are presented in Sec. IV.

### II. EXPERIMENT

#### A. Experimental procedure

The total interaction cross section was determined by relating the number of ions incident on the target to the ions passing the target without interaction. This transmission-type experiment method was described as below.

The experiment was performed at the Institute of Modern Physics in Lanzhou. Secondary radioactive nucleus beams were produced by Radioactive Ion Beam Line in Lanzhou (RIBLL) through the projectile fragmentation of a 60 MeV/nucleon  $^{18}\text{O}$  primary beam accelerated by Heavy Ion Research Facility in Lanzhou (HIRFL). The detector setup is shown in Fig. 1. A diaphragm was used to constrict the beam size. A timing signal from a scintillator at the second focal plane T2 served as the start of a time-to-amplitude converter which was stopped by a signal derived from another scintil-

\*Corresponding author.

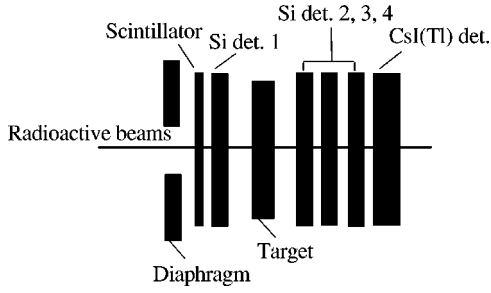


FIG. 1. Detector setup for measuring  $\sigma_R$  of C, N, O isotopes on  $^{12}\text{C}$  target.

lator installed at the first focal plane T1. This provided a measurement of the time-of-flight (TOF) of the incident ions. The first transmission Si surface barrier detector gave their energy losses. Figure 2 is a bidimensional representation of  $\Delta E_1$  versus TOF that enable a direct identification of the incoming ions. Behind the reaction target, a telescope comprised of three transmission Si surface barrier detectors, followed by a CsI(Tl) crystal readout by a photomultiplier was used to identify the noninteracting beam particles. In this experiment, the  $\Delta E$  detectors had thicknesses 300, 300, 1000, and 580  $\mu\text{m}$ , respectively. The thickness of the carbon target was 1 mm. In order to avoid the loss of scattered ions, the four detectors were mounted very compactly and the distance between the reaction target and the telescope was just 2.7 cm.

### B. Data analysis

Due to the energy dependence of the reaction cross section, the accurate determination of the incident ionic energy is required. In the analysis each Si detector was calibrated in energy by Monte Carlo simulation based on the energy-range relationship of energetic ions [13]. In this simulation method, an accurate algorithm for the energy-range relation is expected. The exact description of this relation is very compli-

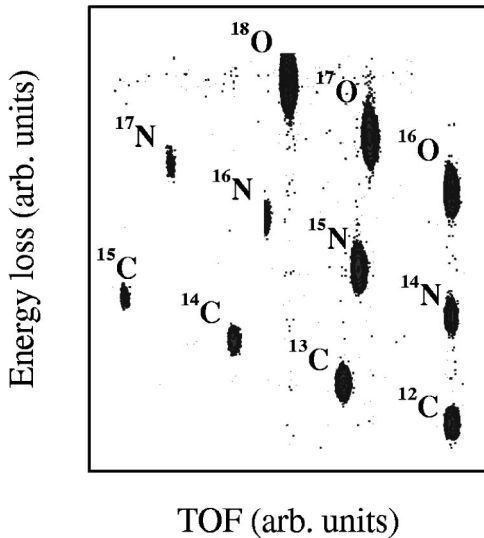


FIG. 2. Bidimensional representation of ( $\Delta E$  versus TOF) particle identification before the target.

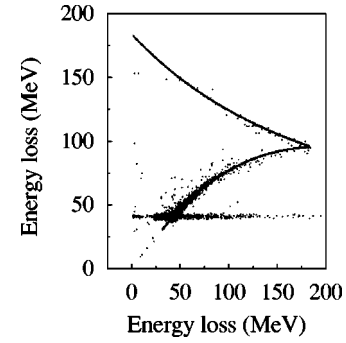


FIG. 3. Correlation plot for two energy losses of the first Si detector and the second Si detector with targetout. The solid line is the band of  $^{17}\text{N}$  by simulation as described in the text, the experimental points after calibration were shown to overlap nicely with the simulated band.

cated. Approximately, the energy-range relation of ions can be described by the following equation [14]:

$$R = \frac{a}{A^{(b-1)}Z^2} E^b, \quad (2)$$

where  $E$  is the kinetic energy of the ion in units of MeV,  $A$  and  $Z$  are the mass and atomic number of the ion, and  $a$  and  $b$  are parameters. But the error becomes larger with the decrease of energy. Calculations show that this error is approximately in inverse proportion to the effective charge of the ion. In order to give a better description of the energy-range relation at low energies, we present a new expression

$$R = \frac{a}{A^{(b-1)}Z^2 \delta^2} E^b, \quad (3)$$

where  $\delta^2 = 1 - \exp[-c - dE/(A^{(b-1)}Z^2)]$  comes from the energy dependence of the effective charge [13,15]. The parameters  $a$ ,  $b$ ,  $c$ , and  $d$  are optimized for  $^{17}\text{N}$  in the calculation by a least-squares fit to the results of TRIM96 [16]. It was shown that Eq. (3) could give a better description of the energy-range relationship of energetic ions than Eq. (2), especially at low energies. Using Eq. (3), the stopping of ions in the detectors could be simulated. A linearity transformation like  $\Delta E_i = k_i(x_i - x_{0i})$ , where  $x_i$  is the channel number of the  $i$ th  $\Delta E$  detector,  $k_i$  and  $x_{0i}$  are constants and  $\Delta E_i$  is the energy loss for the  $i$ th  $\Delta E$  detector after energy calibration expressed in MeV, was made for each  $\Delta E$  detector. Adjusting the constants  $k_i$  and  $x_{0i}$  to make a good overlap between the calibrated experimental points and the simulated bands, we could get good energy calibration for all  $\Delta E$  detectors. In the calibration good overlap was obtained for all the measured isotope bands at the same time. In Fig. 3, the correlation for two energy losses of the first Si detector (300  $\mu\text{m}$ ) and the second Si detector (300  $\mu\text{m}$ ) is displayed. From the figure we can see that the simulation band is in good agreement with the experimental points.

The energy-deposition spectra after the target shown in Fig. 4 was obtained by using TOF and  $\Delta E_1$  gates which select  $^{17}\text{N}$  as the incident ions. Events left to the dotted line

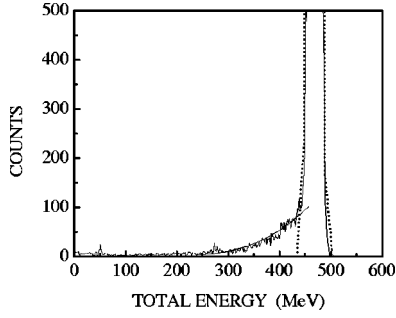


FIG. 4. Energy-deposition spectra of  $^{17}\text{N}$  after the target. The events left of the dotted line near 450 MeV are counted as reaction events which are obtained by a Gaussian fit to the peak.

near 450 MeV are counted as reactions [17]. From this spectra we obtain a probability  $\eta_1$ , defined as the ratio of reactions to total events. The subscript ‘‘1’’ denotes that the reactions take place beyond the first Si detector. The probability  $\eta_2$ , for reactions occurring beyond the second Si detector, was found from the spectra taken with an additional  $\Delta E_2$  energy gate which excludes particles reacting in the target and the second Si detector. The probability  $\eta_3$  was found similarly. Then the reaction cross section in the third Si detector was obtained from the difference between  $\eta_2$  and  $\eta_3$  [17]. The reaction probability in the second Si detector denoted as  $\lambda_2$  can be calculated out from this  $\sigma_R$ . From the difference between  $\eta_1$  and  $\eta_2$ , the reaction probability in the target and the second Si detector denoted as  $\lambda_1$  can be obtained. Finally, we determined  $\sigma_R$  in the carbon target from the difference between  $\lambda_1$  and  $\lambda_2$  which cancels out the reactions in the second Si detector, for details see Ref. [17].

### III. EXPERIMENTAL RESULTS AND DISCUSSION

The  $\sigma_R$  data was presented in Table I. The energy represents the incident ion’s energy in the middle of the carbon target. The errors of  $\sigma_R$  refer to the statistical error plus the mean systematic error ( $\pm 3\%$ ) of extrapolating the reaction events of low- $Q$ -value reactions into the middle of the non-reacted ion’s peak.

Figure 5 shows the comparison of our results with the Glauber model calculation using the same procedure as adopted in Ref. [4]. It can be seen from the figure that the

TABLE I. Total reaction cross section for C, N, O isotopes with  $^{12}\text{C}$  target at intermediate energies.

Projectile	Energy (MeV/nucleon)	$\sigma_R$ (mb)
$^{12}\text{C}$	40.7	$1173 \pm 56$
$^{13}\text{C}$	33.4	$1296 \pm 40$
$^{14}\text{C}$	27.4	$1357 \pm 75$
$^{15}\text{C}$	20.7	$1601 \pm 130$
$^{16}\text{C}$	39.0	$1559 \pm 44$
$^{14}\text{N}$	39.3	$1291 \pm 66$
$^{15}\text{N}$	33.1	$1363 \pm 55$
$^{16}\text{N}$	27.3	$1437 \pm 69$
$^{17}\text{N}$	35.0	$1362 \pm 34$
$^{16}\text{O}$	38.7	$1277 \pm 74$
$^{17}\text{O}$	32.6	$1360 \pm 42$
$^{18}\text{O}$	28.0	$1393 \pm 59$

present data for  $^{12}\text{C}$  and  $^{13}\text{C}$  agree with earlier measurements. The Glauber model underestimates  $\sigma_R$  at intermediate energies for all the nuclei and larger difference between model calculation and the experimental data was shown for  $^{15}\text{C}$ .

In Ref. [4] evidence was shown for the difference factor  $d$  being higher for  $^{15}\text{C}$ , but there is no data for  $^{13}\text{C}$ ,  $^{14}\text{C}$ , and  $^{16}\text{C}$ . In order to see the systematic behavior of  $d$ , we calculated it for the reaction systems measured in the present experiment. The  $(N-Z)$  dependence of  $d$  was given in Fig. 6. For carbon, the results of Ozawa *et al.* was also shown [4].  $d$  from the present experiment for  $^{15}\text{C}$  is also very large and we have added the  $d$  of  $^{15}\text{C}$ ’s neighbor nuclei  $^{13,14,16}\text{C}$  which is very important for the conclusion of the existence of anomalous nuclear structure in  $^{15}\text{C}$ . It can be seen from the figure that  $d$  shows an abnormal increase for  $^{15}\text{C}$ . This supports the assumption of a possible anomalous nuclear structure for  $^{15}\text{C}$ . Due to the nonapplicability of the Glauber model at intermediate energy range, it seems like that  $d$  could be beam-energy dependent. The present data for  $^{15}\text{C}$  was taken at a beam-energy lower than for other isotopes (Table I) and the Glauber calculation could be expected to perform worse, the lower the beam energy, so that there could be larger systematic error for  $^{15}\text{C}$ . But the extraction of nucleon distribution and nuclear radii from the total reaction

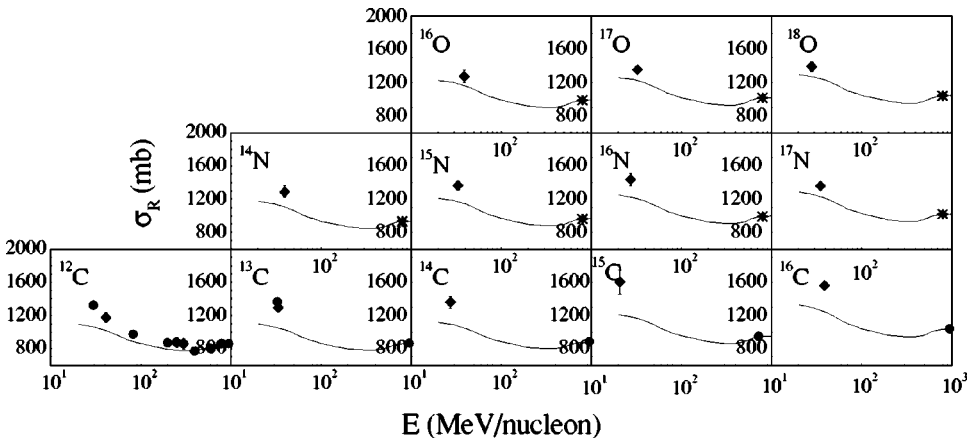


FIG. 5. The energy dependence of  $\sigma_R$  for C, N, O isotopes with carbon target. The solid lines are calculated using the Glauber model along with HO-type density distribution. The present data are indicated by the diamonds. The solid dots are data taken from Refs. [4,5,18], the stars are calculated by the parametrized formula of  $\sigma_R$  [19].

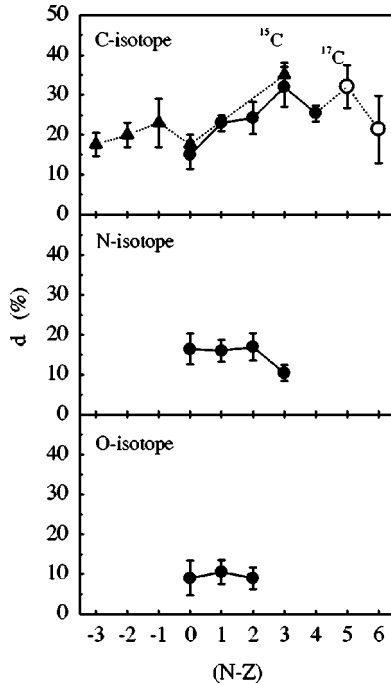


FIG. 6. The  $(N-Z)$  dependence of the difference factor ( $d$ ). The present data are indicated by the solid dots. The triangles are taken from Refs. [4], the open circles are taken from Refs. [22,23]. The experimental  $\sigma_R$  of target other than carbon were normalized to the value with carbon target by using the parametrized formula of  $\sigma_R$  [19].

cross section at both high energies and intermediate energies was done almost exclusively by using the Glauber model. To extract nuclear structure information from the cross section at intermediate energies using the difference factor  $d$  is one of the most important methods at present. It was pointed out that the Boltzmann-Uehling-Uhlenbeck (BUU) calculations can reproduce the experimental total reaction cross section at intermediate energies better than the Glauber calculation [20]. The 10–20% systematical underestimation of  $\sigma_R$  by the Glauber model for normal nuclei was removed out by the BUU calculation. But the difference factor  $d$  of nuclei with an anomalous structure are larger than that of their neighbors both for BUU and Glauber calculation [21]. The results are shown in Fig. 7. For comparison the data from the present experiment was also plotted in this figure. An increase of  $d$  from our experiment by BUU calculation was also shown for  $^{15}\text{C}$  as compared to that of  $^{13,14}\text{C}$ . This suggests that the difference factor is sensitive to the nuclear structure such as the neutron halo or skin. The use of the Glauber model in the analysis of the difference factor would give larger value of  $d$  for the experimental point at lower energies, but should not have much effect on the conclusion. For  $^{17}\text{C}$ , the possible existence of an abnormal nuclear structure is also indicated from other experiments [22,23]. For N and O isotopes which we have measured in this experiment, there is no indication

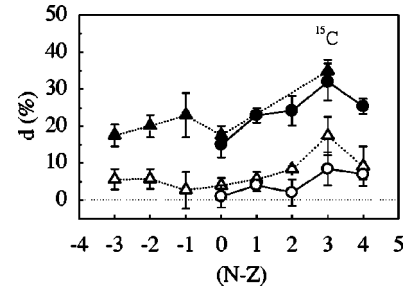


FIG. 7. Isospin dependences of the difference factor ( $d$ ) for C isotope at intermediate energy. The solid uptriangles indicated the data from Ref. [4] by the Glauber calculation. The open triangles are results calculated by BUU model [4,21]. The solid and open circles were the data from the present experiment by the Glauber and BUU calculations, respectively. The curves are to guide the eye. For details of the BUU calculation see Refs. [20,21].

of special nuclear structure since  $d$  is less than 20%, although it varies little for different nuclei. The high-energy data from Ref. [4] indicates that  $^{15}\text{C}$  is of normal size, while the analysis of the cross section at intermediate energy in terms of the difference factor  $d$  demonstrates that  $^{15}\text{C}$  has anomalous structure. To clarify this discrepancy, more experimental measurement of  $\sigma_R$  at more energies points and with more precise methods should be performed.

#### IV. CONCLUSION

In summary, the total reaction cross sections for  $^{12-16}\text{C}$ ,  $^{14-17}\text{N}$ , and  $^{16-18}\text{O}$  at intermediate energies were measured. A method of Monte Carlo simulation based on the energy-range relation of energetic ions for energy calibration of  $\Delta E$  detector was introduced. Comparison of the total reaction cross section with Glauber model calculations was made. Using HO-type density distribution, the Glauber calculation always underestimates the  $\sigma_R$  at intermediate energies. A larger enhancement of  $\sigma_R$  for  $^{15}\text{C}$  was observed than for its neighbors. For  $^{15}\text{C}$ , the abnormal increase of the difference factor  $d$  as compared to its neighbors and the narrow width of momentum distribution [11] support the assumption of its possible anomalous nuclear structure. Further experiments are needed to confirm above conclusions.

#### ACKNOWLEDGMENTS

We would like to thank the members of the RIBLL group and the HIRFL staff for all their help and for the  $^{18}\text{O}$  beam. This work was supported by the Major State Basic Research Development Program under Contract No. G2000 77400, the National Science Foundation of China under Grants No. 19625513 and 19725521, the National Science Foundation of China under Grants No. 19675059 and 19705012, and the Shanghai Science and Technology Development Fund under Grants No. 96XD14011 and 97QA14038.

- [1] I. Tanihata, H. Hamagaki, O. Hashimoto, Y. Shida, N. Yoshikawa, K. Sugimoto, O. Yamakawa, T. Kobayashi, and T. Takahashi, *Phys. Lett.* **160B**, 380 (1985).
- [2] I. Tanihata, H. Hamagaki, O. Hashimoto, Y. Shida, N. Yoshikawa, K. Sugimoto, O. Yamakawa, T. Kobayashi, and N. Takahashi, *Phys. Rev. Lett.* **55**, 2676 (1985).
- [3] I. Tanihata, T. Kobayashi, O. Yamakawa, S. Shimoura, K. Ekuni, K. Sugimoto, T. Takahashi, T. Shimoda, and H. Sato, *Phys. Lett. B* **206**, 592 (1988).
- [4] A. Ozawa, I. Tanihata, T. Kobayashi, Y. Sugahara, O. Yamakawa, K. Omata, K. Sugimoto, D. Olson, W. Christie, and H. Wieman, *Nucl. Phys.* **A608**, 63 (1996), and references therein.
- [5] A. Ozawa, O. Bochkarev, L. Chulkov, D. Cortina, H. Geissel, M. Hellstrom, M. Ivanov, R. Janik, K. Kimura, T. Kobayashi, A. A. Korshennikov, G. Munzenberg, F. Nickel, Y. Ogawa, A. A. Ogloblin, M. Pfutzner, V. Pribora, H. Simon, B. Sitar, P. Strmen, K. Summerer, T. Suzuki, I. Tanihata, M. Winkler, K. Yamashita, and K. Yoshida, RIKEN-AF-NP-294 (1998).
- [6] T. Kobayashi, O. Yamakawa, K. Omata, K. Sugimoto, T. Shimoda, N. Takahashi, and I. Tanihata, *Phys. Rev. Lett.* **60**, 2599 (1988).
- [7] T. Minamisono, T. Ohtsubo, I. Minami, S. Fukuda, A. Kitagawa, M. Fukuda, K. Matsuta, Y. Norji, S. Takeda, H. Sagawa, and H. Kitagawa, *Phys. Rev. Lett.* **69**, 2058 (1992).
- [8] W. Geithner, S. Kappertz, M. Keim, P. Lievens, R. Neugart, L. Vermeeren, S. Wilbert, V. N. Fedoseyev, U. Koster, V. I. Mishin, V. Sebastian, and ISOLDE Collaboration, *Phys. Rev. Lett.* **83**, 3792 (1999).
- [9] R. Anne, R. Bimbot, S. Dogny, H. Emling, D. Guillemaud-Mueller, P.G. Hansen, P. Hornshoj, F. Humbert, B. Jonson, M. Keim, M. Lewitowicz, P. Moller, A. C. Mueller, R. Neugart, T. Nilsson, G. Nyman, F. Pougheon, K. Riisager, M.-G. Saint-Laurent, G. Schrieder, O. Sorlin, O. Tengblad, and K. Wilhelmson Rolander, *Nucl. Phys.* **A575**, 125 (1994).
- [10] T. Nakamura, N. Fukuda, T. Kobayashi, N. Aoi, H. Iwasaki, T. Kubo, A. Mengoni, M. Notani, H. Otsu, H. Sakurai, S. Shimoura, T. Teranishi, Y. X. Watanabe, K. Yoneda, and M. Ishihara, *Phys. Rev. Lett.* **83**, 1112 (1999).
- [11] D. Bazin, W. Benenson, B. A. Brown, J. Brown, B. Davids, M. Fauerbach, P. G. Hansen, P. Mantica, D. J. Morrissey, C. F. Powell, B. M. Sherrill, and M. Steiner, *Phys. Rev. C* **57**, 2156 (1998); D. Bazin, B. A. Brown, J. Brown, M. Fauerbach, M. Hellstrom, S. E. Hirzebruch, J. H. Kelley, R. A. Kryger, D. J. Morrissey, R. Pfaff, C. F. Powell, B. M. Sherrill, and M. Thoennessen, *Phys. Rev. Lett.* **74**, 3569 (1995).
- [12] T. Baumann, M. J. G. Borge, H. Geissel, H. Lenske, K. Markenroth, W. Schwab, M. H. Smedberg, T. Aumann, L. Axelsson, U. Bergmann, D. Cortina-Gil, L. Fraile, M. Hellstrom, M. Ivanov, N. Iwasa, R. Janik, B. Jonson, G. Munzenberg, F. Nickel, T. Nilsson, A. Ozawa, A. Richter, K. Riisager, C. Scheidenberger, G. Schrieder, H. Simon, B. Sitar, P. Strmen, K. Summerer, T. Suzuki, M. Winkler, H. Wollnik, and M. V. Zhukov, *Phys. Lett. B* **439**, 256 (1998).
- [13] D. Q. Fang, J. Feng, X. Z. Cai, J. S. Wang, W. Q. Shen, Y. G. Ma, Y. T. Zhu, S. L. Li, H. Y. Wu, Q. B. Gou, G. M. Jin, W. L. Zhan, Z. Y. Guo, and G. Q. Xiao, *Chin. Phys. Lett.* **16**, 15 (1999).
- [14] E. Bronchalo, L. D. Peral, J. Medina, J. Sequeiros, and N. Hasebe, *Nucl. Instrum. Methods Phys. Res. A* **399**, 65 (1997).
- [15] W. Booth and I. S. Grand, *Nucl. Phys.* **63**, 481 (1965).
- [16] Computer code TRIM, version 96.01, J. P. Biersack and J. F. Ziegler (1996); see also, J. F. Ziegler, J. P. Biersack, and U. Littmark, *The Stopping and Range of Ions in Solids* (Pergamon, New York, 1985).
- [17] R. E. Warner, R. A. Patty, P. M. Voyles, A. Nadasen, F. D. Becchetti, J. A. Brown, H. Esbensen, A. Galonsky, J. J. Kolata, J. Kruse, M. Y. Lee, R. M. Ronningen, P. Schwandt, J. von Schwarzenberg, B. M. Sherrill, K. Subotic, J. Wang, and P. Zecher, *Phys. Rev. C* **54**, 1700 (1996).
- [18] S. Kox, A. Gamp, R. Cherkaoui, A. J. Cole, N. Longequeue, J. Menet, C. Perrin, and J. B. Viano, *Nucl. Phys.* **A420**, 162 (1984); S. Kox, A. Gamp, C. Perrin, J. Arvieux, R. Bertholet, J. F. Brundet, M. Buenerd, R. Cherkaoui, A. J. Cole, Y. El-Masri, N. Longequeue, J. Menet, F. Merchez, and J. B. Viano, *Phys. Rev. C* **35**, 1678 (1987).
- [19] W. Q. Shen, B. Wang, J. Feng, W. L. Zhan, Y. T. Zhu, and E. P. Feng, *Nucl. Phys.* **A491**, 130 (1989).
- [20] Y. G. Ma, W. Q. Shen, J. Feng, and Y. Q. Ma, *Phys. Lett. B* **302**, 386 (1993); *Phys. Rev. C* **48**, 850 (1993).
- [21] X. Z. Cai, W. Q. Shen, J. Feng, D. Q. Fang, Y. G. Ma, Q. M. Su, H. Y. Zhang, and P. Y. Hu, *Chin. Phys. Lett.* (to be published), and references therein.
- [22] A. C. C. Villari, W. Mittig, E. Plagnol, Y. Scutz, M. Lewitowicz, L. Bianchi, B. Fernandez, J. Gastebois, A. Gillbert, C. Stephan, L. Tassan-Got, G. Audi, W. L. Zhan, A. Cunsolo, A. Foti, A. Belazyorov, S. Lukyanov, and Y. Penionzhkevich, *Phys. Lett. B* **268**, 345 (1991).
- [23] M. G. Saint-Laurent, R. Anne, D. Bazin, D. Guillemaud-Mueller, U. Jahnke, G. M. Jin, A. C. Mueller, J. F. Bruandet, F. Glasser, S. Kox, E. Liatard, T. U. Chan, G. J. Costa, C. Heitz, Y. El-Masri, F. Hanappe, R. Bimbot, E. Arnold, and R. Neugart, *Z. Phys. A* **322**, 457 (1989).